

## Articles

## Molecular Oxygen Insertion in Benzylcobaloximes with Mixed Dioximes

Gargi Dutta, Moitree Laskar, and B. D. Gupta\*

Department of Chemistry, Indian Institute of Technology, Kanpur, India 208016

Received September 21, 2007

The complexes  $\text{ArCH}_2\text{Co}(\text{gH})(\text{dpgH})\text{Py}$  have been synthesized and characterized by NMR. Molecular oxygen insertion into the  $\text{Co}-\text{C}$  bond in  $\text{ArCH}_2\text{Co}(\text{L})(\text{dpgH})\text{Py}$  ( $\text{L} = \text{gH}, \text{dmgH}, \text{chgH}$ ) complexes under photochemical conditions forms a mixture of products within 5 min. The equilibration/decomposition of  $\text{ArCH}_2\text{Co}(\text{L})(\text{dpgH})\text{Py}$  to the corresponding  $\text{ArCH}_2\text{Co}(\text{L})_2\text{Py}$  and  $\text{ArCH}_2\text{Co}(\text{dpgH})_2\text{Py}$  complexes and molecular oxygen insertion starts immediately and simultaneously. The ratio of these products changes with time, and finally  $\text{ArCH}_2(\text{O}_2)\text{Co}(\text{L})(\text{dpgH})\text{Py}$  and  $\text{ArCH}_2(\text{O}_2)\text{Co}(\text{dpgH})_2\text{Py}$  are the major products formed. The spectral data are interrelated, and a good correlation is found between  $\Delta\delta_{1\text{H}}(\text{Py}_\alpha)$  and  $\delta^{13\text{C}}(\text{C}=\text{N}_{\text{gH}})$  or  $\delta^{13\text{C}}(\text{C}=\text{N}_{\text{dpgH}})$ , indicating ring current throughout the metallabicyclic. The CV data show that the dioxy complex is easier to reduce than the parent complex. The molecular structure of  $4\text{-Cl-C}_6\text{H}_4\text{CH}_2\text{Co}(\text{dpgH})(\text{gH})\text{Py}$  has been reported.

## Introduction

Since the  $\text{Co}-\text{C}$  bond cleavage is the key step involved in  $\text{B}_{12}$ -dependent enzymatic or cobaloxime mediated reactions, the strength of the  $\text{Co}-\text{C}$  bond as a function of steric and electronic factors of axial as well as equatorial ligands in cobaloximes<sup>28</sup> have been systematically investigated.<sup>1–5</sup> Our recent results, based on spectral and structural studies, have shown that, in addition to the trans effect of the axial base, the cis influence, the effect of the equatorial dioxime on the axial ligands, plays an important role toward the stability of the  $\text{Co}-\text{C}$  bond.<sup>6,7</sup> We have interpreted the spectral correlations using our field effect model.<sup>8</sup> This is an improved and modified version of the previous models of Marzilli and Lopez and works best when

both cobalt anisotropy<sup>9,10</sup> and ring current<sup>11,12</sup> are considered together rather than in isolation from each other. Our similar studies on cobaloximes with mixed dioximes,  $\text{RCo}(\text{dioxime1})-(\text{dioxime2})\text{Py}$ , despite having reduced ring current and cobalt anisotropy, have shown that the spectral data fitted well as per our model. The overall steric cis influence of the dioxime is found to follow the order  $\text{dmstgH} > \text{dpgH} > \text{gH-dpgH} > \text{dmgH-dpgH} > \text{chgH-dpgH} > \text{chgH} > \text{dmgH} > \text{gH}$ .<sup>8,13</sup> The inherently weak  $\text{Co}-\text{C}$  bond in the organocobaloximes undergoes homolytic cleavage with visible light, similar to the activation of vitamin  $\text{B}_{12}$  by apoenzyme.<sup>14</sup> Since  $\text{Co}-\text{C}$  bond cleavage is the key step in many cobaloxime-mediated reactions and the effect of the dioxime is felt most on the  $\text{Co}-\text{CH}_2$  bond, the insertion of molecular oxygen into the  $\text{Co}-\text{C}$  bond has shown that the two effects, steric cis influence and the rate of insertion, are related to each other and follow the same order:  $\text{dmstgH} > \text{dpgH} > \text{chgH} > \text{dmgH} > \text{gH}$ .<sup>15</sup> We wish to further test this concept to see if this order can be expanded to the mixed dioxime complexes as well. A complication, however,

\* To whom correspondence should be addressed. Tel: +91-512-2597046. Fax: +91-512-2597436. E-mail: bdg@iitk.ac.in.

(1) Randaccio, L.; Bresciani-Pahor, N.; Zangrando, E.; Marzilli, L. G. *Chem. Soc. Rev.* **1989**, *18*, 225.

(2) (a) Toscano, P. J.; Marzilli, L. G. *Prog. Inorg. Chem.* **1984**, *104*, 105. (b) Randaccio, L. *Comments Inorg. Chem.* **1999**, *21*, 327. (c) Gupta, B. D.; Roy, S. *Inorg. Chim. Acta* **1988**, *146*, 209.

(3) (a) Yohannes, P. G.; Bresciani-Pahor, N.; Randaccio, L.; Zangrando, E.; Marzilli, L. G. *Inorg. Chem.* **1988**, *27*, 4738. (b) Summers, M. F.; Marzilli, L. G.; Bresciani-Pahor, N.; Randaccio, L. *J. Am. Chem. Soc.* **1984**, *106*, 4478.

(4) (a) Marzilli, L. G.; Gerli, A.; Calafat, A. M. *Inorg. Chem.* **1992**, *31*, 4617. (b) Hirota, S.; Polson, S. M.; Puckett, J. M., Jr.; Moore, S. J.; Mitchell, M. B.; Marzilli, L. G. *Inorg. Chem.* **1996**, *35*, 5646. (c) Polson, S. M.; Cini, R.; Pifferi, C.; Marzilli, L. G. *Inorg. Chem.* **1997**, *36*, 314.

(5) (a) Randaccio, L.; Furlan, M.; Geremia, S.; Slouf, M.; Srnova, I.; Toffoli, D. *Inorg. Chem.* **2000**, *39*, 3403. (b) Randaccio, L.; Geremia, S.; Nardin, G.; Slouf, M.; Srnova, I. *Inorg. Chem.* **1999**, *38*, 4087.

(6) (a) Gupta, B. D.; Qanungo, K. J. *Organomet. Chem.* **1997**, *543*, 125. (b) Gupta, B. D.; Qanungo, K.; Barclay, T.; Cordes, W. *J. Organomet. Chem.* **1998**, *560*, 155.

(7) Gupta, B. D.; Qanungo, K. *J. Organomet. Chem.* **1998**, *557*, 243.

(8) Mandal, D.; Gupta, B. D. *Organometallics* **2005**, *24*, 1501, and references therein.

(9) Trogler, W. C.; Stewart, R. C.; Epps, L. A.; Marzilli, L. G. *Inorg. Chem.* **1974**, *13*, 1564.

(10) Bresciani-Pahor, N.; Forcolin, M.; Marzilli, L. G.; Randaccio, L.; Summers, M. F.; Toscano, P. J. *Coord. Chem. Rev.* **1985**, *63*, 1.

(11) (a) Lopez, C.; Alvarez, S.; Solans, X.; Font-Altaba, M. *Inorg. Chim. Acta* **1986**, *111*, L19. (b) Lopez, C.; Alvarez, S.; Solans, X.; Font-Altaba, M. *Inorg. Chem.* **1986**, *25*, 2962. (c) Alvarez, S.; Vicente, R.; Hoffmann, R. *J. Am. Chem. Soc.* **1985**, *107*, 6253.

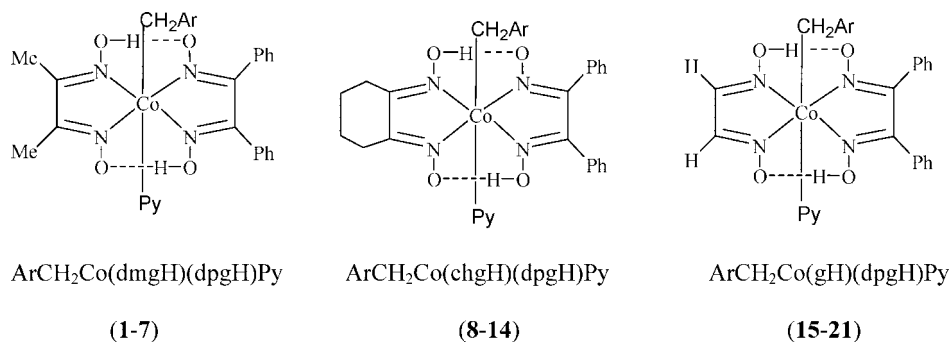
(12) Alvarez, S.; Lopez, C. *Inorg. Chim. Acta* **1982**, *63*, 57.

(13) Gupta, B. D.; Singh, V.; Yamuna, R.; Barclay, T.; Cordes, W. *Organometallics* **2003**, *22*, 2670.

(14) (a) Pratt, J. M.; Whitera, B. R. D. *J. Chem. Soc. A* **1971**, 252. (b) Ramakrishna, D. N.; Symons, M. C. R. *J. Chem. Soc., Faraday Trans. 1* **1984**, 423. (c) Jensen, F.; Madan, V.; Buchnan, D. H. *J. Am. Chem. Soc.* **1971**, *93*, 5285. (d) Brown, K. L. *Dalton Trans.* **2006**, 1123.

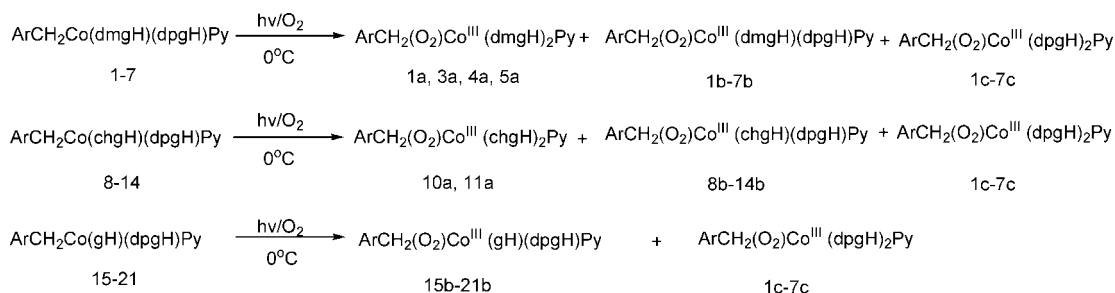
(15) (a) Bhuyan, M.; Laskar, M.; Mandal, D.; Gupta, B. D. *Organometallics* **2007**, *26*, 3559. (b) Gupta, B. D.; Vijaiakanth, V.; Singh, V. *J. Organomet. Chem.* **1998**, *570*, 1.

Scheme 1



Ar=Ph; 4-Cl-C<sub>6</sub>H<sub>4</sub>; 4-CN-C<sub>6</sub>H<sub>4</sub>; 4-OMe-C<sub>6</sub>H<sub>4</sub>; 3-OMe-C<sub>6</sub>H<sub>4</sub>; 2-thienyl; 2-naphthyl

Scheme 2



may arise because the mixed dioxime complexes decompose/equilibrate in solution.<sup>13,16,17</sup>

We have, therefore, carried out molecular oxygen insertion in ArCH<sub>2</sub>Co(dpgH)(dioxime)Py (dioxime = dmgh, chgH, gH) (Schemes 1 and 2), and careful monitoring of the reaction has been performed to determine if the equilibration occurs before or after the insertion. We also report the synthesis of the hitherto unknown ArCH<sub>2</sub>Co(dpgH)(gH)Py complexes, and the X-ray structure of 4-Cl-C<sub>6</sub>H<sub>4</sub>CH<sub>2</sub>Co(dpgH)(gH)Py is described. An electrochemical study on PhCH<sub>2</sub>Co(dpgH)(gH)Py and its dioxy product is also reported.

## Experimental Section

<sup>1</sup>H and <sup>13</sup>C spectra were recorded on a JEOL JNM LAMBDA 400 FT NMR instrument (at 400 MHz for <sup>1</sup>H and at 100 MHz for <sup>13</sup>C) in CDCl<sub>3</sub> solution with TMS as internal standard. The NMR data are reported in ppm. Elemental analysis was carried out at the Regional Sophisticated Instrumentation Center, Lucknow, India, and at IIT Kanpur. UV-vis spectra were recorded on a JASCO V570 spectrophotometer in dry chloroform at 298 K. A Julabo UC-20 low-temperature refrigerated circulator was used to maintain the desired temperature. Glyoxime (*Caution!* glyoxime is highly flammable and explosive when dry), diphenylglyoxime, nioxime, and benzyl halides were purchased from Aldrich and used as such. The syntheses of ArCH<sub>2</sub>Co(dmgh)(dpgH)Py (1-7), ArCH<sub>2</sub>Co(chgH)(dpgH)Py (8-14),<sup>17a,b</sup> and ClCo(gH)(dpgH)Py<sup>17d</sup> have been described before by us. Silica gel (100-200 mesh) and distilled solvents were used in all chromatographic separations. Cyclic voltammetry (CV) measurements were carried out using a BAS Epsilon electrochemical workstation in dichloromethane (dry) at a

concentration of 1 mM of each complex with 0.1 M tetra-*n*-butylammonium hexafluorophosphate (TBAHFPF<sub>6</sub>) as the supporting electrolyte. All the measurements were performed with a BASi platinum-disk or glassy-carbon working electrode; a Ag/AgCl reference electrode (3 M NaCl), and a platinum-wire counter electrode. The reversible ferrocene/ferrocenium ion (Fc/Fc<sup>+</sup>) couple occurs at *E*<sub>1/2</sub> = +0.43(71) V versus the Ag/AgCl electrode under the same experimental conditions. The molar percentages of the species in Figures 1-5 have been calculated from the integration of the <sup>1</sup>H NMR signals of the CH<sub>2</sub> group bound to CoO<sub>2</sub>.

**X-ray Crystal Structure Determination and Refinement.** Orange crystals were obtained by slow evaporation of the solutions of the complex in methanol and dichloromethane. Single-crystal

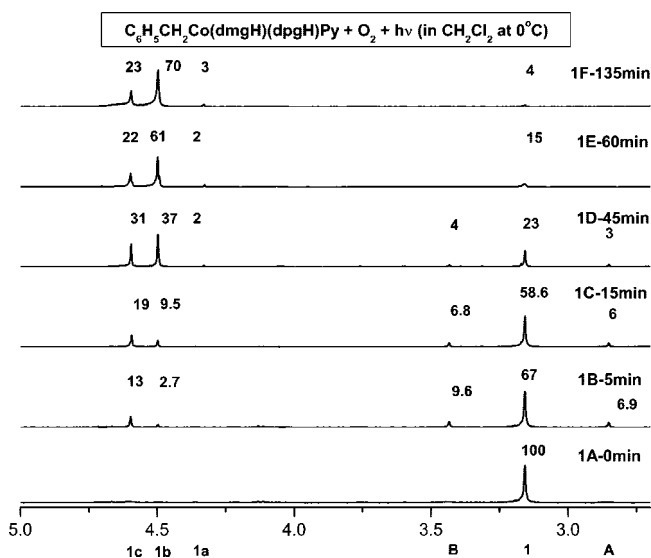


**Figure 1.** Monitoring of oxygen insertion in C<sub>6</sub>H<sub>5</sub>CH<sub>2</sub>Co(dmgh)(dpgH)Py: (A) C<sub>6</sub>H<sub>5</sub>CH<sub>2</sub>Co(dmgh)<sub>2</sub>Py; (B) C<sub>6</sub>H<sub>5</sub>CH<sub>2</sub>Co(dpgH)<sub>2</sub>Py. Numerical labels in the spectra represent the relative proportions in percentages of the products formed during equilibration.

(16) Dodd, D.; Johnson, M. D.; Lockman, B. L. *J. Am. Chem. Soc.* **1977**, *99*, 3664.

(17) (a) Gupta, B. D.; Singh, V.; Qanungo, K.; Vijaikanth, V.; Yamuna, R.; Barclay, T.; Cordes, W. *J. Organomet. Chem.* **2000**, *602*, 1. (b) Gupta, B. D.; Yamuna, R.; Singh, V.; Tiwari, U.; Barclay, T.; Cordes, W. *J. Organomet. Chem.* **2001**, *627*, 80. (c) Gupta, B. D.; Tiwari, U.; Barclay, T.; Cordes, W. *J. Organomet. Chem.* **2001**, *629*, 83. (d) Gupta, B. D.; Yamuna, R.; Mandal, D. *Organometallics* **2006**, *25*, 706.

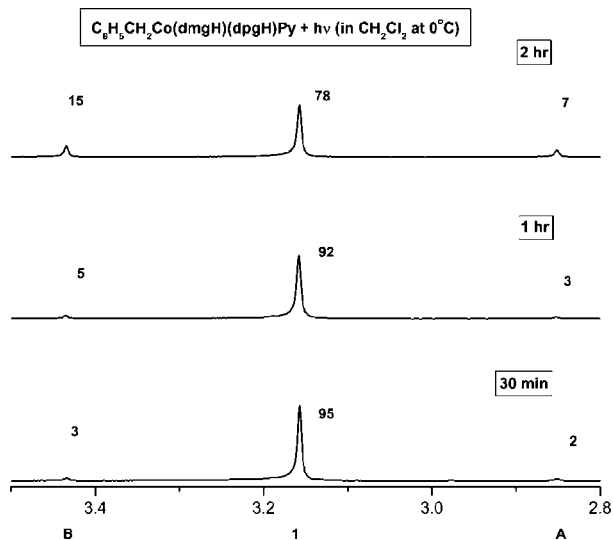


**Figure 2.** Blank reaction 1, equilibration of  $C_6H_5CH_2Co(dmgh)(dpgH)Py$  in dichloromethane at 0 °C under argon: (A)  $C_6H_5CH_2Co(dmgh)_2Py$ ; (B)  $C_6H_5CH_2Co(dpgH)_2Py$ . Numerical labels in the spectra represent the relative proportions in percentages of the products formed during equilibration.

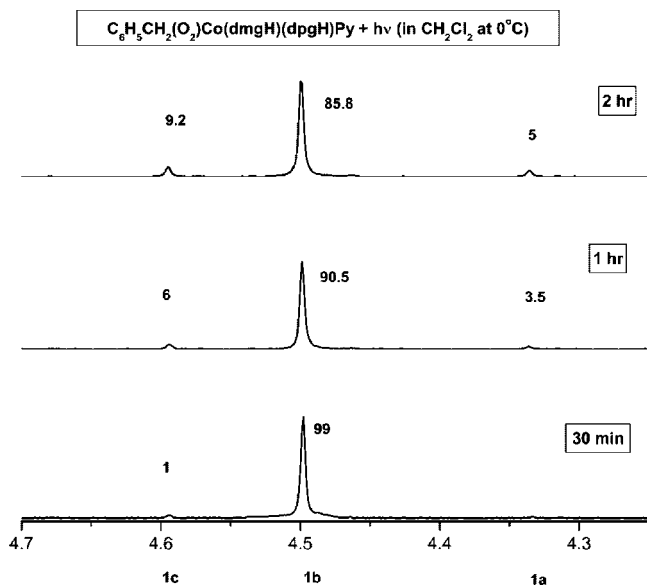


**Figure 3.** Blank reaction 2, equilibration of  $C_6H_5CH_2(O_2)Co(dmgh)(dpgH)Py$  in dichloromethane at 0 °C under argon. Numerical labels in the spectra represent the relative proportions in percentage of the products formed during equilibration.

X-ray data were collected using graphite-monochromated Mo  $K\alpha$  radiation ( $\lambda = 0.71073 \text{ \AA}$ ) at room temperature. Linear absorption coefficients, scattering factors for the atoms, and anomalous dispersion corrections were taken from ref 18. Data integration and reduction were processed with SAINT<sup>19</sup> software. An empirical absorption correction was applied to the collected reflections with SADABS<sup>20</sup> using XPREP.<sup>21</sup> The structure was solved by direct methods using SIR-97<sup>22</sup> and was refined on  $F^2$  by the full-matrix least-squares technique using the SHELXL-97<sup>23</sup> program package. The space group is  $P2_1/n$ . A total of 6701 intensities were measured in the range of 2.35–28.40°, and 3964 were considered as observed, applying the condition  $I > 2\sigma(I)$ . All non-hydrogen atoms were refined with anisotropic displacement parameters. The hydrogen atom positions or thermal parameters were not refined but were included in the structure factor calculations. Pertinent crystal data

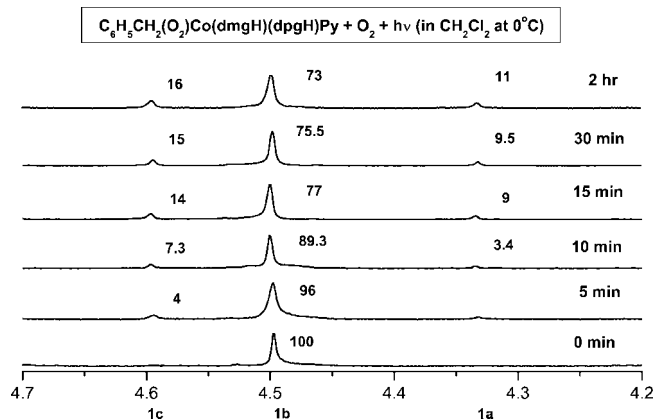


**Figure 4.** Blank reaction 3, equilibration of  $C_6H_5CH_2(O_2)Co(dmgh)(dpgH)Py$  in dichloromethane at 0 °C under oxygen. Numerical labels in the spectra represent the relative proportions in percentages of the products formed during equilibration.

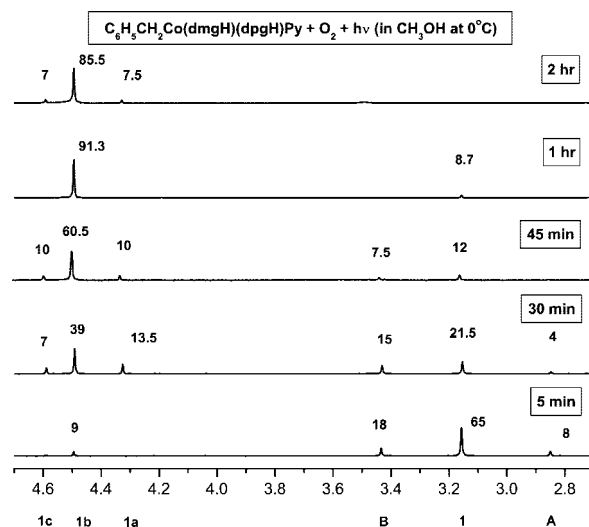


**Figure 5.** Monitoring of oxygen insertion in  $C_6H_5CH_2Co(dmgh)(dpgH)Py$  in methanol: (A)  $C_6H_5CH_2Co(dmgh)_2Py$ ; (B)  $C_6H_5CH_2Co(dpgH)_2Py$ . Numerical labels in the spectra represent the relative proportions in percentages of the products formed during equilibration.

and refinement parameters are compiled in Table 1. The CIF file has been deposited with the Cambridge Crystallographic Data Center, CCDC number 661150. These data can be obtained free of charge from the director, CCDC, 12 Union Road, Cambridge CB2 1EX, U.K. (e-mail, deposit@ccdc.cam.ac.uk; web, <http://www.ccdc.cam.ac.uk>).

**Synthesis of  $ArCH_2Co(gH)(dpgH)Py$  (15–21): General Procedure.** A solution of  $ClCo^{III}(gH)(dpgH)Py$  (0.20 g, 0.40 mmol) in methanol (8 mL) was thoroughly purged with argon and was cooled to 0 °C. The solution turned deep blue on addition of 1 mL of an aqueous solution of NaOH (1 pellet in 2 mL of water)

(18) *International Tables for X-ray Crystallography*, Kynoch Press: Birmingham, England, 1974; Vol. IV.

(19) SAINT+, version 6.02; Bruker AXS, Madison, WI, 1999.

(20) Sheldrick, G. M., SADABS, Empirical Absorption Correction Program; University of Göttingen, Göttingen, Germany, 1997.

(21) XPREP, version 5.1; Siemens Industrial Automation Inc., Madison, WI, 1995.

(22) Altomare, A.; Burla, M. C.; Camalli, M.; Cascarano, G. L.; Giacovazzo, C.; Guagliardi, A.; Moliterni, A. G. G.; Polidori, G.; Spagna, R. *J. Appl. Crystallogr.* **1999**, *32*, 115–119.

(23) Sheldrick, G. M. SHELXL-97, Program for Crystal Structure Refinement; University of Göttingen, Göttingen, Germany, 1997.

**Table 1. Crystal Data and Structure Refinement Details for 16**

|  |   |
|--|---|
| empirical formula  | C <sub>28</sub> H <sub>25</sub> ClCoN <sub>5</sub> O <sub>4</sub> |
| formula wt   | 589.91  |
| temp (K)   | 293   |
| diffraction measurement device/scan method                   | Smart CCD area detector/ $\varphi$ - $\omega$                     |
| cryst syst   | monoclinic  |
| space group  | <i>P</i> 2 <sub>1</sub> / <i>n</i>                                |
| unit cell dimens   |   |
| <i>a</i> (Å)   | 9.885(5)  |
| <i>b</i> (Å)   | 19.138(5)   |
| <i>c</i> (Å)   | 14.544(5)   |
| $\alpha$ (deg)   | 90.000(5)   |
| $\beta$ (deg)  | 100.923(5)  |
| $\gamma$ (deg)   | 90.000(5)   |
| <i>V</i> (Å <sup>3</sup> )                                   | 2701.6(18)  |
| <i>Z</i>   | 4   |
| $\rho$ (calcd) (Mg/m <sup>3</sup> )                          | 1.450   |
| $\mu$ (mm <sup>-1</sup> )                                    | 0.778   |
| <i>F</i> (000)   | 1216  |
| cryst size (mm <sup>3</sup> )                                | 0.30 × 0.25 × 0.22  |
| index ranges   | -13 ≤ <i>h</i> ≤ 8<br>-25 ≤ <i>k</i> ≤ 20<br>-19 ≤ <i>l</i> ≤ 17  |
| no. of rflns collected                                       | 17 574  |
| no. of indep rflns   | 6701  |
| refinement method  | full-matrix least squares on <i>F</i> <sup>2</sup>                |
| GOF on <i>F</i> <sup>2</sup>                                 | 1.05  |
| final <i>R</i> indices ( <i>I</i> > 2 $\sigma$ ( <i>I</i> )) |   |
| <i>R</i> 1   | 0.0616  |
| w <i>R</i> 2   | 0.1226  |
| <i>R</i> indices (all data)                                  |   |
| <i>R</i> 1   | 0.1141  |
| w <i>R</i> 2   | 0.1509  |
| no. of data/restraints/params                                | 6701/0/368  |

**Table 2. Molar Distribution of 15–21<sup>a</sup>**

| compd     | molar distribn (%) |          |
|-----------|--------------------|----------|
|           | <b>c</b>           | <b>b</b> |
| <b>15</b> | 19                 |          |
| <b>16</b> | 13                 | 87       |
| <b>17</b> | 9                  | 91       |
| <b>18</b> | 18                 | 82       |
| <b>19</b> | 16                 | 84       |
| <b>20</b> | 56                 | 44       |
| <b>21</b> | 14                 | 86       |

<sup>a</sup> Legend: **c**, ArCH<sub>2</sub>Co(dpgH)<sub>2</sub>Py; **b**, ArCH<sub>2</sub>Co(gH)(dpgH)Py.

followed by NaBH<sub>4</sub> (0.026 g, 0.7 mmol, dissolved in 0.5 mL of water). Benzyl chloride (0.15 g, 1.18 mmol) in methanol (2 mL) was added dropwise. Acetic acid (1 mL) was added to the reaction vessel after 30 min. The reaction mixture was stirred for another 30 min in the dark, during which time it was brought to ambient temperature and the contents were poured into cold water. The orange-red solid was filtered, dried, and chromatographed on a silica gel column with ethyl acetate/chloroform as the eluents. Two products, PhCH<sub>2</sub>Co<sup>III</sup>(gH)(dpgH)Py (0.15 g, 68%) and PhCH<sub>2</sub>Co<sup>III</sup>-(dpgH)<sub>2</sub>Py (0.04 g, 15%), were isolated. PhCH<sub>2</sub>Co<sup>III</sup>(dpgH)<sub>2</sub>Py came out first with 10% ethyl acetate in chloroform, and PhCH<sub>2</sub>Co<sup>III</sup>(gH)(dpgH)Py eluted with 40–80% ethyl acetate in chloroform. PhCH<sub>2</sub>Co<sup>III</sup>(dpgH)<sub>2</sub>Py was compared with an authentic sample from our laboratory.<sup>17</sup>

**Molecular Oxygen Insertion: General Procedure.** A solution of mixed dioxime complex (0.2 mmol in 20 mL of dichloromethane)

at 0 °C was irradiated with two 200 W tungsten lamps kept at a distance of approximately 10 cm, and pure oxygen gas was bubbled into this solution. The progress of the reaction was monitored by TLC on silica gel using ethyl acetate as the eluent. The reaction was complete within 2 h 30 min in all cases. There was a distinct color change from yellow-orange to dark brown at this stage. At the end of the reaction, the solvent was evaporated and the crude product was purified on the silica gel column using ethyl acetate and chloroform as the eluent. The dioxy dpgH complexes (**1c–7c**) eluted out first with 30% ethyl acetate/70% CHCl<sub>3</sub> mixture followed by the dioxy mixed-ligand complexes (**1b–21b**) with 70% ethyl acetate/30% CHCl<sub>3</sub>. Finally, the dmgH (**1a–7a**) or chgH (**8a–14a**) dioxy complex was eluted with 100% ethyl acetate. The complexes **1a–7a**, **8a–14a**, and **1c–7c** were matched with authentic samples from our laboratory.<sup>17</sup>

**Reaction Monitoring.** Oxygen gas was bubbled through a solution of PhCH<sub>2</sub>Co(dmgH)(dpgH)Py (**1**; 100 mg) in 10 mL of dichloromethane at 0 °C while the solution was irradiated with a 200 W tungsten lamp. The aliquots from the reaction mixture were taken out at time intervals of 5, 15, 45, 60, and 135 min. The aliquot solution was evaporated to dryness, and its NMR spectra were recorded in CDCl<sub>3</sub>.

**Blank Reaction 1.** A solution of PhCH<sub>2</sub>Co(dmgH)(dpgH)Py (**1**; 20 mg in 2 mL of dichloromethane) at 0 °C was irradiated with a 200 W tungsten lamp while argon gas was continuously bubbled through the solution. The aliquots were taken out at time intervals of 0.5, 1, and 2 h. The aliquot solution was evaporated to dryness, and its NMR spectra were recorded in CDCl<sub>3</sub>.

**Blank Reaction 2.** This was carried out as in blank reaction 1, except that the solution of the dioxy compound PhCH<sub>2</sub>(O<sub>2</sub>)-Co(dmgH)(dpgH)Py (**1b**; 20 mg in 2 mL of dichloromethane) was irradiated under argon.

**Blank Reaction 3.** This was carried out as in blank reaction 2, except that the dioxy complex PhCH<sub>2</sub>(O<sub>2</sub>)Co(dmgH)(dpgH)Py (**1b**; 20 mg in 2 mL of dichloromethane) was irradiated under oxygen and the aliquots were taken out at time intervals of 5, 10, 15, 30, and 120 min.

**Blank Reaction 4.** Oxygen gas was continuously bubbled through a solution of PhCH<sub>2</sub>Co(dmgH)(dpgH)Py (**1**; 100 mg in 10 mL of methanol) at 0 °C while the solution was irradiated with a 200 W tungsten lamp. Aliquots from the reaction mixture were taken out at time intervals of 5, 30, 45, 60, and 120 min.

## Results and Discussion

**Synthesis.** The mixed dioxime cobalt complexes were unknown until recently.<sup>13,16,17</sup> We have already reported the synthesis of RCo(dioxime)(dpgH)Py<sup>13,17a,b</sup> [(R = alkyl, benzyl; dioxime = dmgH, chgH). For example, the reaction of Co<sup>I</sup>(dmgH)(dpgH)Py or Co<sup>I</sup>(chgH)(dpgH)Py, generated in situ by the sodium borohydride reduction of the corresponding chlorocobaloxime, with alkyl halide always formed a mixture of three products, ArCH<sub>2</sub>Co(dmgH)<sub>2</sub>Py or ArCH<sub>2</sub>Co(chgH)<sub>2</sub>Py, ArCH<sub>2</sub>-Co(dmgH)(dpgH)Py or ArCH<sub>2</sub>Co(chgH)(dpgH)Py, and ArCH<sub>2</sub>-Co(dpgH)<sub>2</sub>Py, in different proportions. Scrambling led to the cross products. We have proposed a reaction scheme on the basis of many independent reactions.<sup>17a,b</sup> In the present case, under similar conditions, a mixture of only two products, ArCH<sub>2</sub>-Co(gH)(dpgH)Py and ArCH<sub>2</sub>Co(dpgH)<sub>2</sub>Py, is formed in the

**Table 3. Molar Distribution of 1–21<sup>a</sup>**

| fraction | molar distribn (%) |          |          |          |          |          |          |          |          |           |           |           |           |           |           |           |           |           |           |           |           |  |
|----------|--------------------|----------|----------|----------|----------|----------|----------|----------|----------|-----------|-----------|-----------|-----------|-----------|-----------|-----------|-----------|-----------|-----------|-----------|-----------|--|
|          | <b>1</b>           | <b>2</b> | <b>3</b> | <b>4</b> | <b>5</b> | <b>6</b> | <b>7</b> | <b>8</b> | <b>9</b> | <b>10</b> | <b>11</b> | <b>12</b> | <b>13</b> | <b>14</b> | <b>15</b> | <b>16</b> | <b>17</b> | <b>18</b> | <b>19</b> | <b>20</b> | <b>21</b> |  |
| <b>a</b> | 10                 |          | 13       | 9        | 9        |          |          |          |          | 10        | 8         |           |           |           |           |           |           |           |           |           |           |  |
| <b>b</b> | 71                 | 82       | 73       | 54       | 81       | 78       | 91       | 91       | 91       | 72        | 82        | 92        | 85        | 95        | 92        | 97        | 97        | 85        | 86        | 45        | 76        |  |
| <b>c</b> | 19                 | 18       | 14       | 37       | 10       | 22       | 9        | 9        | 9        | 18        | 10        | 8         | 15        | 5         | 8         | 3         | 3         | 15        | 14        | 55        | 24        |  |

<sup>a</sup> Legend: **a**, ArCH<sub>2</sub>(O<sub>2</sub>)Co(L)<sub>2</sub>Py; **b**, ArCH<sub>2</sub>(O<sub>2</sub>)Co(L)(dpgH)Py; **c**, ArCH<sub>2</sub>(O<sub>2</sub>)Co(dpgH)<sub>2</sub>Py; L, dmgH or chgH or gH.

Table 4. <sup>1</sup>H NMR Data (ppm) for 15–21<sup>a</sup>

| compd     | aromatic                     | –CH <sub>2</sub> (s) | ligand |                      | pyridine |       |              | OH⋯O (s) |
|-----------|------------------------------|----------------------|--------|----------------------|----------|-------|--------------|----------|
|           |                              |                      | gH(s)  | dpgH (m)             | α (d)    | γ (t) | β (t)        |          |
| <b>15</b> | 6.74 (d) <sup>b</sup>        | 3.20                 | 7.49   | 7.10–7.26            | 8.70     | 7.78  | 7.38         | 18.31    |
| <b>16</b> | 6.76 (d), 7.06 (d)           | 3.11                 | 7.49   | 7.16–7.26            | 8.67     | 7.79  | 7.39         | 18.28    |
| <b>17</b> | 6.73 (d) <sup>b</sup>        | 3.07                 | 7.50   | 7.16–7.28            | 8.65     | 7.79  | 7.39         | 18.23    |
| <b>18</b> | 6.66 (d), 6.78 (d)           | 3.03                 | 7.46   | 7.12–7.20            | 8.70     | 7.77  | 7.37         | 18.31    |
| <b>19</b> | 6.76 (t), 6.87 (d), 7.03 (t) | 3.18                 | 7.50   | 7.12–7.22            | 8.70     | 7.78  | 7.38         | 18.30    |
| <b>20</b> | 6.9–7.03 <sup>b</sup>        | 3.36                 | 7.39   | 7.18–7.35            | 8.62     | 7.82  | 7.39         | 18.61    |
| <b>21</b> | 6.99 (t), 7.12 (t)           | 3.36                 | 7.52   | 7.30–7.43, 7.58–7.70 | 8.71     | 7.78  | <sup>b</sup> | 18.34    |

<sup>a</sup> OMe appears at 3.73 for **4b** and 3.67 for **5b**. <sup>b</sup> Merge with dpgH; free Py appears at 8.57 (α), 7.05 (β), and 7.43 (γ).

Table 5. <sup>1</sup>H NMR Data (ppm) for 1b–7b

| compd                 | aromatic (m) | –CH <sub>2</sub> (s) | ligand   |              | pyridine |       |              | OH⋯O (s) |
|-----------------------|--------------|----------------------|----------|--------------|----------|-------|--------------|----------|
|                       |              |                      | dmgH (s) | dpgH (m)     | α (d)    | γ (t) | β (t)        |          |
| <b>1b</b>             | 7.08–7.24    | 4.50                 | 2.31     | <sup>a</sup> | 8.54     | 7.73  | 7.29         | 18.61    |
| <b>2b</b>             | 7.08–7.27    | 4.43                 | 2.33     | <sup>a</sup> | 8.54     | 7.75  | 7.31         | 18.58    |
| <b>3b</b>             | 7.07–7.28    | 4.50                 | 2.34     | <sup>a</sup> | 8.53     | 7.76  | 7.32         | 18.58    |
| <b>4b<sup>b</sup></b> | 6.70–7.29    | 4.42                 | 2.32     | <sup>a</sup> | 8.54     | 7.73  | <sup>a</sup> | 18.58    |
| <b>5b<sup>b</sup></b> | 6.72–7.23    | 4.48                 | 2.32     | <sup>a</sup> | 8.55     | 7.74  | 7.30         | 18.57    |
| <b>6b</b>             | 6.82–6.85    | 4.63                 | 2.35     | 7.14–7.25    | 8.54     | 7.74  | 7.29         | 18.54    |
| <b>7b</b>             | 7.00–7.68    | 4.65                 | 2.31     | <sup>a</sup> | 8.57     | 7.75  | 7.31         | 18.65    |

<sup>a</sup> Merge with aromatic. <sup>b</sup> 4-OMe appears at 3.75 (s) and 3-OMe at 3.67 (s).

Table 6. <sup>1</sup>H NMR Data (ppm) for 8b–14b

| compd                  | aromatic (m) | –CH <sub>2</sub> (s) | ligand             |               | pyridine |              |              | OH⋯O (s) |
|------------------------|--------------|----------------------|--------------------|---------------|----------|--------------|--------------|----------|
|                        |              |                      | chgH               | dpgH          | α (d)    | γ (t)        | β (t)        |          |
| <b>8b</b>              | 7.09–7.24    | 4.49                 | 2.95 (d), 2.75 (d) | <sup>a</sup>  | 8.56     | 7.75         | 7.31         | 18.31    |
| <b>9b</b>              | 7.00–7.25    | 4.30                 | 2.96 (d), 2.76 (d) | <sup>a</sup>  | 8.55     | 7.75         | 7.31         | 18.31    |
| <b>10b</b>             | 7.08–7.47    | 4.51                 | 2.93 (d), 2.80 (d) | <sup>a</sup>  | 8.54     | 7.77         | <sup>a</sup> | 18.29    |
| <b>11b<sup>b</sup></b> | 6.71–7.25    | 4.42                 | 2.97 (d), 2.76 (d) | <sup>a</sup>  | 8.56     | 7.75         | 7.31         | 18.30    |
| <b>12b<sup>b</sup></b> | 6.71–7.24    | 4.48                 | 2.96 (d), 2.76 (d) | <sup>a</sup>  | 8.55     | 7.74         | 7.30         | 18.32    |
| <b>13b</b>             | 6.83–6.86    | 4.63                 | 3.01 (d), 2.78 (d) | 7.14–7.25 (m) | 8.55     | 7.75         | 7.30         | 18.25    |
| <b>14b</b>             | 7.00–7.76    | 4.66                 | 2.96 (d), 2.76 (d) | <sup>a</sup>  | 8.58     | <sup>a</sup> | <sup>a</sup> |          |

<sup>a</sup> Merge with aromatic; <sup>b</sup> 4-OMe appears at 3.75 and 3-OMe at 3.67 (s).

Table 7. <sup>1</sup>H NMR Data (ppm) for 15b–21b

| compd                  | aromatic (m) | –CH <sub>2</sub> (s) | ligand |              | pyridine |       |              | OH⋯O (s) |
|------------------------|--------------|----------------------|--------|--------------|----------|-------|--------------|----------|
|                        |              |                      | gH(s)  | dpgH         | α (d)    | γ (t) | β (t)        |          |
| <b>15b</b>             | 7.08–7.24    | 4.54                 | 7.60   | <sup>a</sup> | 8.53     | 7.77  | 7.33         | 18.39    |
| <b>16b</b>             | 7.08–7.30    | 4.47                 | 7.60   | <sup>a</sup> | 8.51     | 7.78  | 7.34         | 18.37    |
| <b>17b</b>             | 7.09–7.47    | 4.56                 | 7.61   | <sup>a</sup> | 8.51     | 7.80  | <sup>a</sup> | 18.41    |
| <b>18b<sup>b</sup></b> | 6.71–7.25    | 4.46                 | 7.60   | <sup>a</sup> | 8.53     | 7.78  | 7.33         | 18.39    |
| <b>19b<sup>b</sup></b> | 6.71–7.25    | 4.52                 | 7.58   | <sup>a</sup> | 8.50     | 7.74  | 7.30         | 18.41    |
| <b>20b</b>             | 6.71–7.25    | 4.53                 | 7.60   | <sup>a</sup> | 8.52     | 7.84  | <sup>a</sup> | 18.42    |
| <b>21b</b>             | 7.09–7.53    | 4.56                 | 7.61   | <sup>a</sup> | 8.51     | 7.80  | <sup>a</sup> | 18.41    |

<sup>a</sup> Merge with aromatic. <sup>b</sup> 4-OMe appears at 3.75 and 3-OMe at 3.65 (s).

reaction of Co<sup>I</sup>(gH)(dpgH)Py with the benzylic halide. No trace of the corresponding gH complex ArCH<sub>2</sub>Co(gH)<sub>2</sub>Py is formed. The major product formed, however, is the required complex (**15b–21b**). The molar ratios are given in Table 2. In the synthesis of the gH/dpgH complexes, the addition of acetic acid before the aqueous workup is essential, since it prevents the decomposition of the weakly acidic glyoxime hydrogen under alkaline conditions and thereby increases the yield of the product.

The mechanism of the reaction is similar to that of the dmgH–dpgH or chgH–dpgH combination described earlier and might involve the randomization of the equatorial dioxime ligand along with alkyl transfer in the presence of cobaloximes (I).<sup>13,16,17</sup> <sup>1</sup>H NMR data are given in Tables 4–7. Elemental analysis and <sup>13</sup>C NMR data are given in the Supporting Information (Tables S1 and S3–S7).

**Oxygen Insertion.** The general characteristics point to the free radical nonchain nature of the reaction. The reaction stops

as soon as the irradiation is stopped. The reaction of molecular oxygen with **1–21** in dichloromethane at 0 °C under irradiation occurs smoothly and is complete in about 2 h. Two products, ArCH<sub>2</sub>(O<sub>2</sub>)Co(L)(dpgH)Py (**1b–21b**) and ArCH<sub>2</sub>(O<sub>2</sub>)Co(dpgH)<sub>2</sub>Py (**1c–7c**), are formed in each reaction. An additional product, ArCH<sub>2</sub>(O<sub>2</sub>)Co(dmgh)<sub>2</sub>Py or ArCH<sub>2</sub>(O<sub>2</sub>)Co(chgH)<sub>2</sub>Py, is also formed in a few cases in the reactions with dmgh/dpgH and chgH/dpgH complexes (**1–14**). The major product, however, is the expected **1b–21b** in all the reactions. The molar distribution of these products is given in Table 3.

The formation of ArCH<sub>2</sub>(O<sub>2</sub>)Co(dmgh)<sub>2</sub>Py, ArCH<sub>2</sub>(O<sub>2</sub>)Co(chgH)<sub>2</sub>Py, and ArCH<sub>2</sub>(O<sub>2</sub>)Co(dpgH)<sub>2</sub>Py is surprising and points to the equilibration of the mixed dioxime complex in solution, before or after the oxygen insertion. In order to sort this out, some independent reactions were carried out. The progress of the reactions was monitored with <sup>1</sup>H NMR over a period of 2 h. The rationale is based on the formation of various

products at different intervals of time.  $\text{PhCH}_2\text{Co}(\text{dmgH})(\text{dpgH})\text{Py}$  (**1**) is taken as a case study.

1. Six compounds were formed in the reaction mixture after 5 min (Figure 1: 1B). This means that the equilibration of  $\text{PhCH}_2\text{Co}(\text{dmgH})(\text{dpgH})\text{Py}$  (**1**) with  $\text{PhCH}_2\text{Co}(\text{dmgH})_2\text{Py}$  (**A**),  $\text{PhCH}_2\text{Co}(\text{dpgH})_2\text{Py}$  (**B**), and  $\text{PhCH}_2\text{Co}(\text{dmgH})(\text{dpgH})\text{Py}$  (**1**) and the insertion of oxygen into these complexes starts simultaneously and immediately. The amount of  $\text{PhCH}_2(\text{O}_2)\text{Co}(\text{dmgH})_2\text{Py}$  (**1a**) formed is slight (2–3%) and remains constant until the end of the reaction. However, the amount of  $\text{PhCH}_2(\text{O}_2)\text{Co}(\text{dpgH})_2\text{Py}$  (**1c**) varies with time. It first increases up to 45 min and then decreases after that. This may be because the insertion is faster in the  $\text{dpgH}$  complexes, as we know from our earlier studies.<sup>15</sup>

2. The ratios of the equilibrated compounds **1a–c**, however, do not match with those in the blank reaction (see point 5). This is because the rate of equilibration is fast in the presence of oxygen (see point 6).

3. The total amount of **1c** formed does not match with the amount of  $\text{PhCH}_2\text{Co}(\text{dpgH})_2\text{Py}$  produced by the equilibration of **1** (Figure 1: 1B–1D). This is because the insertion is faster in  $\text{PhCH}_2\text{Co}(\text{dpgH})_2\text{Py}$  (**B**) as compared to that in  $\text{PhCH}_2\text{Co}(\text{dmgH})(\text{dpgH})\text{Py}$  (**1**) or  $\text{PhCH}_2\text{Co}(\text{dmgH})_2\text{Py}$  (**A**), thus disturbing the equilibrium.<sup>15</sup> After about 45 min, when almost all the  $\text{PhCH}_2\text{Co}(\text{dpgH})_2\text{Py}$  (**B**) has been consumed, the insertion in  $\text{PhCH}_2\text{Co}(\text{dmgH})(\text{dpgH})\text{Py}$  (**1**) becomes more conspicuous, thus decreasing the ratio of  $\text{PhCH}_2(\text{O}_2)\text{Co}(\text{dpgH})_2\text{Py}$  (**1c**) to  $\text{PhCH}_2(\text{O}_2)\text{Co}(\text{dmgH})(\text{dpgH})\text{Py}$  (**1b**) (Figure 1: 1E, 1F).

4. In the blank reaction 1 under argon,  $\text{PhCH}_2\text{Co}(\text{dmgH})(\text{dpgH})\text{Py}$  (**1**) is seen to decompose and three products,  $\text{PhCH}_2\text{Co}(\text{dmgH})_2\text{Py}$  (**A**),  $\text{PhCH}_2\text{Co}(\text{dpgH})_2\text{Py}$  (**B**), and  $\text{PhCH}_2\text{Co}(\text{dmgH})(\text{dpgH})\text{Py}$  (**1**), are observed after 2 h in a 15:78:7 ratio (Figure 2). This distribution, however, changes in the presence of oxygen (see point 1).

5. The blank reaction 2 under argon shows that  $\text{PhCH}_2(\text{O}_2)\text{Co}(\text{dmgH})(\text{dpgH})\text{Py}$  (**1b**) also decomposes, though slowly. Three products,  $\text{PhCH}_2(\text{O}_2)\text{Co}(\text{dmgH})_2\text{Py}$  (**1a**),  $\text{PhCH}_2(\text{O}_2)\text{Co}(\text{dmgH})(\text{dpgH})\text{Py}$  (**1b**), and  $\text{PhCH}_2(\text{O}_2)\text{Co}(\text{dpgH})_2\text{Py}$  (**1c**), are observed at the end of 2 h (Figure 3).

6.  $\text{PhCH}_2(\text{O}_2)\text{Co}(\text{dmgH})(\text{dpgH})\text{Py}$  (**1b**) equilibrates under oxygen (blank reaction 3) to three products,  $\text{PhCH}_2(\text{O}_2)\text{Co}(\text{dmgH})_2\text{Py}$  (**1a**),  $\text{PhCH}_2(\text{O}_2)\text{Co}(\text{dmgH})(\text{dpgH})\text{Py}$  (**1b**), and  $\text{PhCH}_2(\text{O}_2)\text{Co}(\text{dpgH})_2\text{Py}$  (**1c**), in an 11:73:16 ratio. The equilibration occurs quickly, and no significant change occurs after 15 min of the reaction (Figure 4).

7. The reaction in methanol (blank reaction 4) gives information similar to that in point 1. Six products are formed within 5 min (Figure 5), but  $\text{PhCH}_2(\text{O}_2)\text{Co}(\text{dmgH})(\text{dpgH})\text{Py}$  (**1b**) is the major product after 1 h. This then equilibrates **1a–c** in 2 h. The ratio of the products, however, is different in dichloromethane.

It is quite clear from the above observations and conclusions drawn under each point that the mixed dioxime complexes as well as their dioxy products are not stable in solution and readily undergo decomposition/equilibration. Many parallel reactions, including decomposition and oxygen insertion, occur simultaneously in solution. Since the scrambling of the dioxime ligand would require the dissociation of one of the dioxime ligands, the reaction in methanol leads to even faster equilibration. However, we have not been able to isolate any stable intermediate in these reactions.

**Spectroscopy.** <sup>1</sup>H NMR data for **15–21**, **1b–7b**, **8b–14b**, and **15b–21b** are given in Tables 4–7, respectively. <sup>1</sup>H and <sup>13</sup>C NMR resonances are easily assigned on the basis of chemical shifts, and the assignments are consistent with the

related and previously described cobaloximes  $\text{RCo}(\text{dioxime})(\text{dpgH})\text{Py}$  (dioxime =  $\text{dmgH}$ ,  $\text{chgH}$ ).<sup>17</sup>  $\text{Py}_\gamma$ ,  $\text{C}=\text{N}$  ( $\text{gH}$ ), and  $\text{Py}_\alpha$ ,  $\text{C}=\text{N}$  ( $\text{dpgH}$ ) resonances occur close to each other. In the former case, the high-intensity peak is assigned to  $\text{C}=\text{N}$  ( $\text{gH}$ ) (2H attached to 2C) and the low-intensity peak to  $\text{Py}_\gamma$  (1H attached to 1C), whereas in the latter, the high-intensity peak is assigned to  $\text{Py}_\alpha$  (2H attached to 2C) and the low-intensity peak to  $\text{C}=\text{N}$  ( $\text{dpgH}$ ). The assignment has been confirmed by <sup>1</sup>H–<sup>13</sup>C correlation experiments (Supporting Information, Figure S3).  $\text{Py}_\gamma$  and  $\text{C}=\text{N}$  ( $\text{gH}$ ) are merged together in some compounds.

In recent years we have explained the <sup>1</sup>H and <sup>13</sup>C NMR data in  $\text{RCo}(\text{dioxime})_2\text{Py}$  and  $\text{RCo}(\text{dioxime})(\text{dpgH})\text{Py}$  (dioxime =  $\text{dmgH}$ ,  $\text{chgH}$ ; R = alkyl), in terms of cis and trans influence.<sup>8,13,17</sup> Therefore, instead of discussing the detailed interpretation of the data, we highlight only the salient features in  $\text{RCo}(\text{gH})(\text{dpgH})\text{Py}$  (**15–21**). The following observations are noteworthy in the present study. (a) O–H⋯O chemical shifts lie between those of their parent cobaloximes  $\text{ArCH}_2\text{Co}(\text{gH})_2\text{Py}$  and  $\text{ArCH}_2\text{Co}(\text{dpgH})_2\text{Py}$  and also appear consistently upfield by about 0.15–0.20 ppm than the corresponding value in  $\text{ArCH}_2\text{Co}(\text{dmgH})(\text{dpgH})\text{Py}$ . The O–H⋯O resonance follows the order  $\text{dmgstgH} > \text{dpgH} > \text{dmgH-dpgH} > \text{gH-dpgH} > \text{chgH-dpgH} \approx \text{dmgH} > \text{gH} > \text{chgH}$ . (b) Since the chemical shifts of  $\text{CH}_2$  and  $\text{Py}_\alpha$  are affected by the dioxime ring current, it is expected that the values should lie between the parent cobaloximes because of the reduced ring current in the present systems. This is what is observed as well. The overall order for  $\text{Py}_\alpha$  is  $\text{dmgstgH}$ ,  $\text{dpgH} > \text{gH-dpgH} > \text{dmgH-dpgH}$ ,  $\text{chgH-dpgH} > \text{chgH} > \text{dmgH} > \text{gH}$ , and for  $\text{CH}_2$  it is  $\text{dmgstgH}$ ,  $\text{dpgH} > \text{gH-dpgH} > \text{dmgH-dpgH}$ ,  $\text{chgH-dpgH} > \text{gH} > \text{chgH} > \text{dmgH}$ . The mixed-ligand complexes fit well into the order and lend support to the previous finding in  $\text{RCo}(\text{dioxime})_2\text{Py}$  complexes.<sup>6–8,13</sup> The  $\text{Py}_\alpha$  proton is close to O–H⋯O and gets affected by its strength. The stronger the hydrogen bond, the more upfield the  $\text{Py}_\alpha$  resonance.: for example, for  $\text{PhCH}_2\text{Co}(\text{gH})_2\text{Py}$ ,  $\text{Py}_\alpha$  8.54 ppm and O–H⋯O 17.67 ppm; for  $\text{PhCH}_2\text{Co}(\text{dpgH})_2\text{Py}$ ,  $\text{Py}_\alpha$  8.85 ppm and O–H⋯O 18.68 ppm; for  $\text{PhCH}_2\text{Co}(\text{gH})(\text{dpgH})\text{Py}$ ,  $\text{Py}_\alpha$  8.70 ppm and O–H⋯O 18.31 ppm.

In general, a significant upfield shift of about 0.2 ppm is observed for the equatorial protons when the axial alkyl group is replaced with the benzyl group in the cobaloximes (Supporting Information, Table S7). For example, the  $\text{gH}$  proton is shifted upfield (0.2 ppm) in  $\text{ArCH}_2\text{Co}(\text{gH})_2\text{Py}$  (7.24 ppm) as compared to  $\text{EtCo}(\text{gH})_2\text{Py}$  (7.44 ppm), and the same is observed in the  $\text{dmgH}$  complexes as well. The upfield shift can be due to three factors: (a) increased ring current in the metallacycle when alkyl is replaced with the benzyl group (if this is so, then this should affect the  $\text{Py}_\alpha$  proton resonance), (b) decrease in cobalt anisotropy, and (c) the presence of a weak C–H– $\pi$  interaction between the benzyl ring and the dioxime protons (this is absent in the alkylcobaloximes).

An identical value of  $\delta_{\text{H}}(\text{Py}_\alpha)$  and  $\delta_{\text{C}}(\text{C}=\text{N})$  in the alkyl and benzyl complexes would mean that factors a and b do not contribute to the upfield shift. Factor c gains support from X-ray data, where such a C–H– $\pi$  interaction has been observed in the benzyl cobaloximes.<sup>24</sup> This concept also works well when applied to the mixed dioxime complexes; for example, the  $\text{dmgH}$  (Me) in  $\text{ArCH}_2\text{Co}(\text{dmgH})(\text{dpgH})\text{Py}$  appears upfield from that for  $\text{EtCo}(\text{dmgH})(\text{dpgH})\text{Py}$ . However, in the present study the  $\text{gH}$  protons have identical chemical shifts in  $\text{ArCH}_2\text{Co}(\text{gH})(\text{dpgH})\text{Py}$  and  $\text{EtCo}(\text{gH})(\text{dpgH})\text{Py}$ . This is quite surprising and suggests the absence of a C–H– $\pi$  interaction between

(24) (a) Mandal, D.; Gupta, B. D. *Organometallics* **2006**, *25*, 3305. (b) Mandal, M.; Gupta, B. D. *Organometallics* **2007**, *26*, 658.

the benzyl and gH protons. This interaction, however, can not be ascertained, as the benzyl group is oriented over the dpGH wing and not over the gH wing.

The insertion of oxygen brings further changes in the NMR spectra:<sup>29</sup> for example, the O–H···O (0.15 ppm) and CH<sub>2</sub> resonances (1.5 ppm in <sup>1</sup>H and 40–45 ppm in <sup>13</sup>C spectra) appear downfield and the Py<sub>α</sub> resonance appears upfield (0.15 ppm) in **1b–21b** as compared to those in the parent complexes, **1–21**. Similarly, C=N moves downfield by 1.5–2.5 ppm. Furthermore, the order dmGH–dpGH > gH–dpGH > chGH–dpGH for the O–H···O resonance in **1–21** remains the same as in **1b–21b**.

**Correlation.**  $\delta_{13\text{C}}(\text{C}=\text{N}_{\text{gH,dpGH}})$  always appears upfield in **15b–21b** as compared to the corresponding  $\delta_{13\text{C}}(\text{C}=\text{N})$  value in the free dioxime, gH or dpGH. The field effect in the metallabicyclic for different dioximes keeping the same axial R group can be understood by comparing the coordination shifts,  $\Delta\delta_{13\text{C}}(\text{C}=\text{N})$ .<sup>30</sup>  $\Delta\delta_{13\text{C}}(\text{C}=\text{N}_{\text{gH}})$  in **15b–21b** is much higher (7–7.5 ppm) as compared to the corresponding value ( $\Delta\delta_{13\text{C}}(\text{C}=\text{N}_{\text{dmGH}})$ ) (4–4.5 ppm) or  $\Delta\delta_{13\text{C}}(\text{C}=\text{N}_{\text{dmGH}})$  (2–2.5 ppm) in ArCH<sub>2</sub>Co(L)(dpGH)Py (L = dmGH, chGH) (Supporting Information, Table S8). This means that the field effect is significantly higher in the gH–dpGH complexes as compared to the similar mixed dioxime complexes with dgH–dpGH and chGH–dpGH combinations. This supports our previous findings in the alkyl mixed dioxime<sup>17d</sup> complexes and suggests further that this may be the general picture that holds true for all organocobaloximes, irrespective of the nature of the R group and the dioxime.

$\delta_{13\text{C}}(\text{C}=\text{N}_{\text{gH}})$  or  $\delta_{13\text{C}}(\text{C}=\text{N}_{\text{dpGH}})$  correlate well with  $\Delta\delta_{1\text{H}}(\text{Py}_\alpha)$  for the ArCH<sub>2</sub>Co(gH)(dpGH)Py (**15–21**) and XCo(gH)(dpGH)Py (X = Cl, Br, NO<sub>2</sub>, N<sub>3</sub>) complexes.<sup>19</sup> Four values of the inorganic mixed dioxime complexes are included to increase the versatility of the correlation. The negative slope for eq 1 indicates that the  $\Delta\delta_{1\text{H}}(\text{Py}_\alpha)$  and  $\delta_{13\text{C}}(\text{C}=\text{N}_{\text{gH}})$  values are affected in opposite directions. The following correlations suggests the presence of ring current throughout the Co-(dioxime)<sub>2</sub><sup>+</sup> metallabicyclic. This supports our previous results in the alkyl mixed dioxime complexes and further lends support to our field effect model.

$$\delta_{13\text{C}}(\text{C}=\text{N}_{\text{gH}}) = 139.03 - 8.86[\Delta\delta_{1\text{H}}(\text{Py}_\alpha)];$$

$$r^2 = 0.96, \text{ esd} = 0.234 \quad (1)$$

$$\delta_{13\text{C}}(\text{C}=\text{N}_{\text{dpGH}}) = 152.64 + 10.306[\Delta\delta_{1\text{H}}(\text{Py}_\alpha)];$$

$$r^2 = 0.96, \text{ esd} = 0.228 \quad (2)$$

**X-ray Crystal Structure.** We could obtain single crystals of **16** from the slow diffusion of methanol and dichloromethane

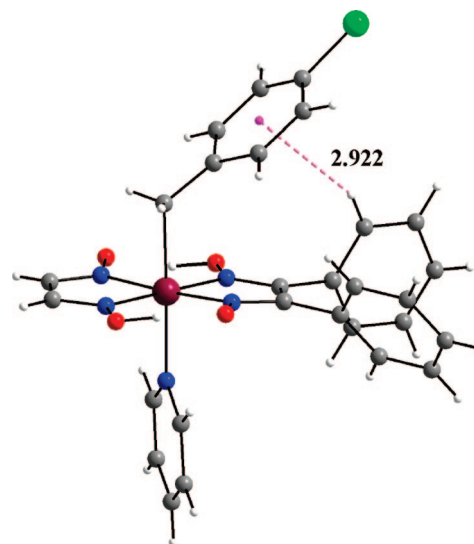


**Figure 6.** Molecular structure of **16**.

solution. The X-ray analysis of the crystals showed the composition as 4-Cl-C<sub>6</sub>H<sub>4</sub>CH<sub>2</sub>Co(gH)(dpGH)Py. A Diamond diagram of the molecular structure of **16** is shown in Figure 6. Selected bond lengths and bond angles are given in Table 8.

The cobalt atom is linked to four nitrogen atoms belonging to the equatorial plane; two nitrogen atoms belong to the dpGH ligand and the other two to the gH ligand. The Co atom displays an approximately octahedral coordination and deviates by 0.026 Å from the mean equatorial N<sub>4</sub> plane. The deviation is toward pyridine, as observed in many structures, and is much smaller as compared to that for the alkyl derivative octylCo(gH)(dpGH)py (0.0383 Å).<sup>17d</sup> Interestingly, EtCo(gH)(dpGH)py contains two molecules in its asymmetric unit with *d* values of –0.0326 and 0.0128 Å. The negative sign means that the deviation is toward the alkyl group.

The pyridine ring is parallel to the glyoxime C–C bonds, its conformation being defined by a twist angle ( $\tau$ )<sup>25</sup> of 76.98°. This is much smaller in octylCo(gH)(dpGH)Py<sup>17d</sup> (88.08°), and the values in PhCH<sub>2</sub>Co(dmGH)(dpGH)Py and PhCH<sub>2</sub>Co(chGH)(dpGH)Py are 80.3(5) and 79.0(3)°, respectively.<sup>17b</sup> There are no significant differences in the Co–N<sub>5</sub> and Co–C bond distances from those in the alkylCo(gH)(dpGH)Py complexes. However, the Co–C–C bond angle is much lower (120.11 (3)°) as compared to that in octylCo(gH)(dpGH)py (125.6°). This is due to the CH– $\pi$  interaction (2.922 Å) between the benzyl and the equatorial dioxime, which is absent in the alkyl derivative. We believe that this interaction must have led to the higher butterfly bending angle ( $\alpha = 5.30^\circ$ )<sup>26</sup> in **16**. This is the largest angle among all the previously reported mixed dioxime cobaloxime complexes.

**Electrochemical Study (Cyclic Voltammetry).** The redox behavior of PhCH<sub>2</sub>Co(gH)(dpGH)Py (**15**) and PhCH<sub>2</sub>(O<sub>2</sub>)Co(gH)(dpGH)Py (**15b**) was examined by cyclic voltammetry (CV). Both compounds display only two redox responses (Supporting Information, Figure S4) within the potential range scanned being –1.6 to +1.6 V vs SCE. While the oxidative response is well-behaved, the reductive response is ill-defined. We assign reversible to quasi-reversible oxidative responses at 1.06 V (**15**) and 1.26 V (**15b**) as due to Co<sup>IV</sup>/Co<sup>III</sup> and the irreversible reductive responses at –0.97 V (**15**) and –0.93 V (**15b**) as due to Co<sup>III</sup>/Co<sup>II</sup> redox processes, respectively. A comparison of the current heights of two responses strengthens our hypotheses. This behavior could be explained as due to either a poorer

(25) The torsion angle ( $\tau$ ) is the angle between two virtual planes that bisects the cobaloxime plane. Each plane is formed by considering the middle point of the C–C bond of two oxime units that passes through cobalt and pyridine nitrogen.

(26) The dihedral angle (butterfly bending angle,  $\alpha$ ) is the angle between two dioxime planes of each cobaloxime unit.

(27) (a) Elliott, C. M.; Hershenhart, E.; Finke, R. G.; Smith, B. L. *J. Am. Chem. Soc.* **1981**, *103*, 5558. (b) Asaro, F.; Dreos, R.; Nardin, G.; Pellizer, G.; Peressini, S.; Randaccio, L.; Siega, P.; Trauzher, G.; Tavagnacco, C. *J. Organomet. Chem.* **2000**, *601*, 114. (c) Bard, A. J.; Faulkner, L. R. *Electrochemical Methods: Fundamentals and Applications*; Wiley: New York, 2001. (d) Singh, A. K.; Mukherjee, R. N. *Dalton Trans.* **2008**, 260.

(28) Cobaloximes have the general formula RCo(L)<sub>2</sub>B, where R is an organic group  $\sigma$ -bonded to cobalt, B is an axial base trans to the organic group, and L is a monoanionic dioxime ligand (e.g., glyoxime (gH), dimethylglyoxime (dmGH), 1,2-cyclohexanedione dioxime (chGH), diphenylglyoxime (dpGH), and dimesityl glyoxime (dmstGH)).

(29) The dioxo products show a characteristic band around 250–260 nm for Co<sup>IV</sup>-dioxime in the UV–vis spectra.

(30)  $\Delta\delta_{13\text{C}}(\text{C}=\text{N}) = \delta(\text{C}=\text{N complex}) - \delta(\text{C}=\text{N free dioxime})$ .

Table 8. Selected Bond Lengths, Bond Angles, and Structural Data for **16** and **X1–X4**<sup>a</sup>

|  | <b>16</b>   | <b>X1</b>  | <b>X2</b>  | <b>X3</b>              | <b>X4</b> |
|--|-------------|------------|------------|------------------------|-----------|
| <i>d</i> (Å)                             | 0.026       | 0.024(2)   | 0.044(2)   | −0.0326, 0.0128        | 0.0383    |
| $\tau$ (deg)                             | 76.983(110) | 80.3(5)    | 79.0(3)    | 88.80, 73.68           | 88.88     |
| $\alpha$ (deg)                           | 5.30        | 4.90       | 3.8        | 0.93, 5.03             | 0.85      |
| Co–N <sub>ax</sub> (Å)                   | 2.056(3)    | 2.086(4)   | 2.070(3)   | 2.0619(18), 2.0720(17) | 2.066(5)  |
| Co–C <sub>ax</sub> /Cl <sub>ax</sub> (Å) | 2.040(4)    | 2.045(60)  | 2.063(4)   | 2.022(2), 2.018(2)     | 2.028(7)  |
| C–Co–N <sub>ax</sub> (deg)               | 177.32(14)  | 175.56(22) | 177.63(15) | 177.48(8), 176.18(9)   | 178.1(3)  |
| Co–C–C <sub>ax</sub> (deg)               | 120.11(3)   | 118.54     | 116.76     | 117.64(15), 119.09(19) | 125.6(6)  |
| C–H··· $\pi$ (Å)                         | 2.922       |            | 2.790      |                        |           |

<sup>a</sup> Legend: **X1**, C<sub>6</sub>H<sub>5</sub>CH<sub>2</sub>Co(dmgh)(dpgH)Py; **X2**, C<sub>6</sub>H<sub>5</sub>CH<sub>2</sub>Co(chgH)(dpgH)Py; **X3**, EtCo(gH)(dpgH)Py; **X4**, (octyl)Co(gH)(dpgH)Py.

thermodynamic stability of the one-electron-reduced species or to the very fast solvolysis reactions of the one-electron-reduced species.<sup>27a,b</sup> The nature of reductive waves points toward the existence of a chemical process following electron transfer (EC mechanism).<sup>27c</sup> Constant-potential (V vs SCE) electrolysis of **15** confirms that it is a one-electron-reduction process (potential applied −1.6 V, *n* = 1.3 (*n* = number of electron passed per molecule)). In the CV scan of **15b** it seems that two reduction peaks are present; however, actually this is not so. This manifestation is due to the EC mechanism. Due to enhanced  $\sigma$  donation by the R<sup>−</sup> group the Co<sup>III</sup> state in **15** and **15b** is substantially stabilized.<sup>27d</sup> In other words, in the present complexes the Co<sup>III</sup>/Co<sup>II</sup> redox process is considerably cathodically shifted. Due to this, the Co<sup>II</sup>/Co<sup>I</sup> redox response is further cathodically shifted and therefore is not observed even down to −1.5 V. The redox behavior of the mixed dioxime complex (**15**) is different from that of the parent complexes C<sub>6</sub>H<sub>5</sub>CH<sub>2</sub>Co(gH)<sub>2</sub>Py and C<sub>6</sub>H<sub>5</sub>CH<sub>2</sub>Co(dpgH)<sub>2</sub>Py. The latter is more nucleophilic than **15**, whereas the former is more difficult to oxidize as well as difficult to reduce as compared to **15** (Supporting Information, Table S10).

### Conclusion

Molecular oxygen insertion into the Co–C bond in 21 complexes, ArCH<sub>2</sub>Co(L)(dpgH)Py (L = gH, dmgh, chgH),

under photochemical conditions forms a mixture of products within 5 min, and the ratios of the products change during the course of reaction; finally, ArCH<sub>2</sub>(O<sub>2</sub>)Co(L)(dpgH)Py and ArCH<sub>2</sub>(O<sub>2</sub>)Co(dpgH)<sub>2</sub>Py are formed as the major products. The equilibration of ArCH<sub>2</sub>Co(L)(dpgH)Py to the corresponding ArCH<sub>2</sub>Co(L)<sub>2</sub>Py and ArCH<sub>2</sub>Co(dpgH)<sub>2</sub>Py complexes and molecular oxygen insertion are the competing reactions. The hitherto unknown ArCH<sub>2</sub>Co(gH)(dpgH)Py complexes have been synthesized and characterized by NMR, and the X-ray structure of 4-Cl-C<sub>6</sub>H<sub>4</sub>CH<sub>2</sub>Co(dpgH)(gH)Py has been described.  $\delta^{13}\text{C}$  (C=N<sub>gH</sub>) or  $\delta^{13}\text{C}$  (C=N<sub>dpgH</sub>) values correlate well with the  $\Delta\delta^1\text{H}$  (Py $\alpha$ ) value and confirm the presence of ring current throughout the metallabicyclic. The dioxy complex is easier to reduce than the parent complex, as observed in a CV study.

**Acknowledgment.** We thank the DST (No. SR/S1/IC-12/2004) New Delhi, India, for financial support. We thank Prof. R. N. Mukherjee for discussion of CV data. We also thank Ms. Preeti Chadha for help in some experiments.

**Supporting Information Available:** Tables and figures giving CHN analysis data, representative <sup>1</sup>H spectra, <sup>13</sup>C NMR data, and cyclic voltammetry data for compounds **15** and **15b**. This material is available free of charge via the Internet at <http://pubs.acs.org>.

OM700938W